

A Dual Scale Approach to Modeling Sub-Filter Velocities due to Shear-Induced Instabilities

A. Goodrich*, and M. Herrmann
School for Engineering of Matter, Transport and Energy
Arizona State University
Tempe, AZ 85287-6106 USA

Abstract

A method to compute sub-filter velocities due to shear induced instabilities on a liquid-gas interface for use in a dual scale LES-DNS model is presented. The method reconstructs the sub-filter velocity field as the sum of a prescribed base velocity profile and a perturbation velocity field determined by the Orr-Sommerfeld equations. The base velocity profile is approximated as an error function appropriately scaled with flow parameters, and the perturbation velocity field is computed by solving the Orr-Sommerfeld equations with appropriate boundary and interface conditions. The perturbation velocities of the Orr-Sommerfeld equations are expanded into Chebyshev polynomials to create a linear eigenvalue problem as outlined by Schmid and Henningson (2001). Finally the eigenvalue problem is solved using a standard linear algebra package and used to evaluate the perturbation velocities. The Chebyshev method is tested under a variety of flow parameters and initial interface disturbances. Results are presented and compared against prior literature and asymptotic solutions.

*Corresponding Author: acgoodri@asu.edu

Introduction

Direct Numerical Simulations of turbulent liquid-gas interfaces require tremendous computational resources to fully resolve all the relevant scales of motion [1]. Primary atomization is governed by the fine scales of motion and instabilities that occur on this interface. To ease the computational burden, a model is required to make predictive simulations feasible.

Several attempts have been proposed to model the unclosed terms in the Large Eddy Simulation (LES) governing equations [2, 3]. Many of these models neglect the geometry and instabilities of the sub-filter interface. A Dual-Scale model is proposed in [4] and a model for the sub-filter shear driven instabilities is presented here.

Governing Equations

The governing equations for an unsteady, incompressible, two-fluid system in the absence of surface tension are the Navier-Stokes equations,

$$\frac{\partial \rho \mathbf{u}}{\partial t} + \nabla \cdot (\rho \mathbf{u} \otimes \mathbf{u}) = -\nabla p + \nabla \cdot (\mu (\nabla \mathbf{u} + \nabla^T \mathbf{u})), \quad (1)$$

where \mathbf{u} is the fluid velocity, ρ is the density, p is the pressure, and μ is the dynamic viscosity. Surface tension is neglected simply to focus attention on the shear driven instabilities of the interface. In addition to the momentum equation, the conservation of mass constrains the velocity field to be divergence-free.

$$\nabla \cdot \mathbf{u} = 0 \quad (2)$$

In the incompressible regime, fluid properties are taken to be uniform throughout each fluid. ρ and μ can therefore be evaluated with a volume-of-fluid scalar, ψ as,

$$\rho = \psi \rho_l + (1 - \psi) \rho_g, \quad (3)$$

$$\mu = \psi \mu_l + (1 - \psi) \mu_g, \quad (4)$$

where the l and g subscripts indicate fluid properties in liquid and gas respectively. ψ is evaluated as $\psi = 0$ in the gas and $\psi = 1$ in the liquid. In addition ψ must also be transported with the flow field as,

$$\frac{\partial \psi}{\partial t} = -\mathbf{u} \cdot \nabla \psi \quad (5)$$

Filtered Governing Equations

Following the methodology of LES modeling, a spatial filter is applied to Eqs. (1) and (2),

$$\begin{aligned} \frac{\partial \bar{\rho} \bar{\mathbf{u}}}{\partial t} + \nabla \cdot (\bar{\rho} \bar{\mathbf{u}} \otimes \bar{\mathbf{u}}) &= -\nabla \bar{p} \\ &+ \nabla \cdot (\bar{\mu} (\nabla \bar{\mathbf{u}} \otimes \nabla^T \bar{\mathbf{u}})) \\ &+ \boldsymbol{\tau}_1 + \nabla \cdot (\boldsymbol{\tau}_2 + \boldsymbol{\tau}_3), \quad (6) \\ \nabla \cdot \bar{\mathbf{u}} &= 0, \quad (7) \end{aligned}$$

where the overbar ($\bar{\cdot}$) implies spatial filtering, and

$$\boldsymbol{\tau}_1 = \frac{\partial \bar{\rho} \bar{\mathbf{u}}}{\partial t} - \frac{\partial \rho \mathbf{u}}{\partial t} \quad (8)$$

$$\boldsymbol{\tau}_2 = \bar{\rho} \bar{\mathbf{u}} \otimes \bar{\mathbf{u}} - \overline{\rho \mathbf{u} \otimes \mathbf{u}} \quad (9)$$

$$\boldsymbol{\tau}_3 = \overline{\mu (\nabla \mathbf{u} + \nabla^T \mathbf{u})} - \bar{\mu} (\nabla \bar{\mathbf{u}} + \nabla^T \bar{\mathbf{u}}) \quad (10)$$

where $\boldsymbol{\tau}_1$, $\boldsymbol{\tau}_2$ and $\boldsymbol{\tau}_3$ represent the sub-filter effects due to acceleration, advection and viscosity respectively[3]. Applying the spatial filter to Eqs. (3) and (4) yields

$$\bar{\rho} = \rho_l \bar{\psi} + \rho_g (1 - \bar{\psi}), \quad (11)$$

$$\bar{\mu} = \mu_l \bar{\psi} + \mu_g (1 - \bar{\psi}), \quad (12)$$

where the spatially filtered ψ is

$$\bar{\psi} = \int \mathcal{G}(\mathbf{x}) \psi d\mathbf{x}. \quad (13)$$

The Dual-Scale Approach to Modeling Sub-filter Shear Driven Instabilities

In place of applying the spatial filter to Eq. (5) and generating a model for the sub-filter terms, the Dual-Scale approach proposed in [4] maintains a fully resolved realization of the interface geometry using the Refined Local Surface Grid (RLSG) method as described in [5]. Under this approach the fully resolved volume-of-fluid scalar ψ is transported as described in Eq. (5), and subsequently filtered according to Eq. (13).

This approach provides an exact closure to any sub-filter terms that arise from filtering Eq. (5), and instead shifts the modeling problem to maintaining a fully resolved interface geometry and correctly predicting the sub-filter motion. The fully resolved velocity field \mathbf{u} can be decomposed into its filtered and sub-grid components, $\mathbf{u} = \bar{\mathbf{u}} + \mathbf{u}_{sg}$. Substituting into Eq. (5) yields

$$\frac{\partial \psi}{\partial t} = -(\bar{\mathbf{u}} + \mathbf{u}_{sg}) \cdot \nabla \psi, \quad (14)$$

leaving only \mathbf{u}_{sg} requiring modeling. [4] proposes to decompose the sub-grid velocity \mathbf{u}_{sg} further into

$$\mathbf{u}_{sg} = \mathbf{u}' + \delta \mathbf{u} + \mathbf{u}_\sigma + \mathbf{u}_g, \quad (15)$$

where \mathbf{u}' is the sub-grid turbulent velocity, $\delta\mathbf{u}$ is the sub-grid shear driven velocity, \mathbf{u}_σ is the sub-grid surface tension velocity and \mathbf{u}_g is the sub-grid accelerational instabilities. The sub-grid turbulent velocity and sub-grid surface tension models are discussed in other works, and the focus of this work is on the sub-grid shear driven velocity, $\delta\mathbf{u}$.

Sub-grid Shear Driven Velocity Model

We propose to model the sub-grid shear driven velocity by use of the Orr-Sommerfeld equations to construct a linear stability problem as outlined in [6]. Within an LES grid cell the error function will be used to approximate the base velocity profile

$$U_g(y) = U_g^* \text{erf}(y/\delta_g) \quad (16)$$

$$U_l(y) = U_l^* \text{erf}(y/\delta_l) \quad (17)$$

where $U_{g/l}^*$ is the asymptotic velocity away from the interface for gas and liquid respectively, y is the direction normal to the interface and $\delta_{g/l}$ is the boundary layer thickness for gas and liquid respectively. The asymptotic velocities and boundary layer thicknesses are constrained at by the continuity of shear stress at the interface via

$$\frac{\mu_l U_l^*}{\delta_l} = \frac{\mu_g U_g^*}{\delta_g}. \quad (18)$$

For brevity of the Orr-Sommerfeld equations we introduce the following non-dimensional parameters: density ratio $r = \rho_g/\rho_l$, viscosity ratio $m = \mu_g/\mu_l$, boundary layer thickness ratio $n = \delta_g/\delta_l$, Reynold's number $\text{Re} = \rho_g U_g^* \delta_g / \mu_g$ and Weber number $\text{We} = \rho_g (U_g^*)^2 \delta_g / \sigma$. Perturbations to the base flow are evaluated by constructing stream functions,

$$\psi_k(x, y, t) = \exp(i\alpha(x - ct)) \phi_k(y) \quad (19)$$

where k denotes liquid or gas, ψ_k is the stream function in either phase, α is the wavenumber of perturbed interface, c is the complex phase speed of the interface, and ϕ_k denotes the y -dependence of the streamfunction. Using the streamfunction definition, the perturbation velocities can be recovered as

$$u = \frac{\partial \psi_k}{\partial y} \quad (20)$$

$$v = -\frac{\partial \psi_k}{\partial x}. \quad (21)$$

The Orr-Sommerfeld equations can then by con-

structed as

$$(U_g - c)(D^2 - \alpha^2)\phi_g - D^2 U_g \phi_g = \frac{1}{i\alpha \text{Re}} (D^2 - \alpha^2)^2 \phi_g \quad (22)$$

$$(U_l - c)(D^2 - \alpha^2)\phi_l - D^2 U_l \phi_l = \frac{r}{m} \frac{1}{i\alpha \text{Re}} (D^2 - \alpha^2)^2 \phi_l \quad (23)$$

where D is the partial derivative with respect to y [6]. At the upper and lower boundaries the tangential perturbation velocities vanish:

$$\phi_g(L_g) = D\phi_g(L_g) = 0 \quad (24)$$

$$\phi_l(-L_l) = D\phi_l(-L_l) = 0. \quad (25)$$

At location of the interface the normal and tangential perturbation velocities are continuous:

$$D\phi_g(0) + \frac{DU_g(0)\phi_g(0)}{c} = D\phi_l(0) + \frac{DU_l(0)\phi_l(0)}{c}, \quad (26)$$

$$\phi_g(0) = \phi_l(0). \quad (27)$$

Finally, the normal and tangential stress must be continuous at the interface:

$$m \left(D^2 \phi_g(0) + \alpha^2 \phi_g(0) + \frac{D^2 U_g(0)\phi_g(0)}{c} \right) = D^2 \phi_l(0) + \alpha^2 \phi_l(0) + \frac{D^2 U_l(0)\phi_l(0)}{c}, \quad (28)$$

$$\begin{aligned} & \frac{m}{i r \alpha \text{Re}} (D^3 \phi_g - 3\alpha^2 D\phi_g) + (c D\phi_g + D U_g \phi_g) \\ & - \frac{1}{i r \alpha \text{Re}} (D^3 \phi_l - 3\alpha^2 D\phi_l) - \frac{1}{r} (c D\phi_l + D U_l \phi_l) \\ & = -\frac{\alpha^2}{r \text{We}} \left(\frac{\phi_l}{c} \right). \end{aligned} \quad (29)$$

Numerical Methods

Eqs. (22) - (29) define an eigenvalue problem for the growth rates and corresponding perturbation velocities of the two fluid system. The eigenfunctions ϕ_k are expanded with Chebyshev polynomials and solved with a collocation algorithm per [7]. Upon reconstructing the sub-grid velocity field near the interface with the RLSC method, Eq. (14) is solved using an unsplit geometric transport scheme for the volume-of-fluid scalar. The geometric interface within each computational cell is accomplished with a PLIC reconstruction with the analytical formulas [8] and surface normal vectors estimated by ELVIRA [9].

The geometric unsplit method ensures that both volume is conserved and that ψ remains bounded under the constraint that divergence-free face-centered velocities are used. Since the eigenvalue problem in [6] was formulated for a flat interface, the eigenfunctions, $\phi_k(y)$, can be used without a coordinate shift. However, if the interface is perturbed then, since y is the normal distance from the perturbed interface, the eigenfunctions must shift vertically by an amount equal to the displacement of the interface. Thus the streamfunctions are not guaranteed to generate divergence-free perturbed velocities in the shifted frame.

To correct this, δu is projected into the subspace of divergence-free velocity fields using the projection step of a standard fractional step method. For the simplicity of the examples presented in this work, the Poisson system is constructed for the entire domain. However, in future work and in keeping with the Dual-Scale methodology, the Poisson system will be constructed only within each LES cell containing an interface.

Results

In the first verification test, a liquid-gas interface is perturbed with a single wavenumber disturbance as shown in Figure (1).

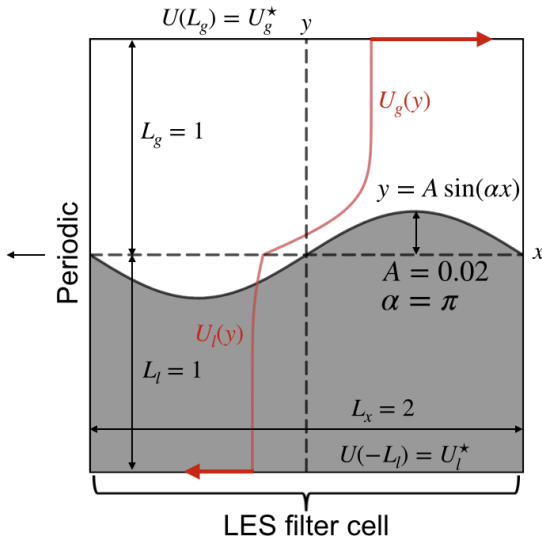


Figure 1. Liquid-gas interface disturbed with a single wavenumber.

The interface is perturbed with a sinusoidal function of the form $y = 0.01 \sin(\pi x)$. The flow parameters of the simulation are provided in table (1).

The advancement of the interface geometry is

Re	We	r	m	δ_g	n	U_g^*
8000	∞	1	0.1	0.25	1	1

Table 1. Simulation flow parameters.

then simulated in three ways: first with a DNS initialized by the perturbation velocities of the eigenvalue problem and allowed to advance without further modeling, next with the perturbation velocities used to advect the volume-of-fluid scalar (referred to as the linear model from here on) and finally with a sine wave growing exponentially with the computed growth rate of the eigenvalue problem.

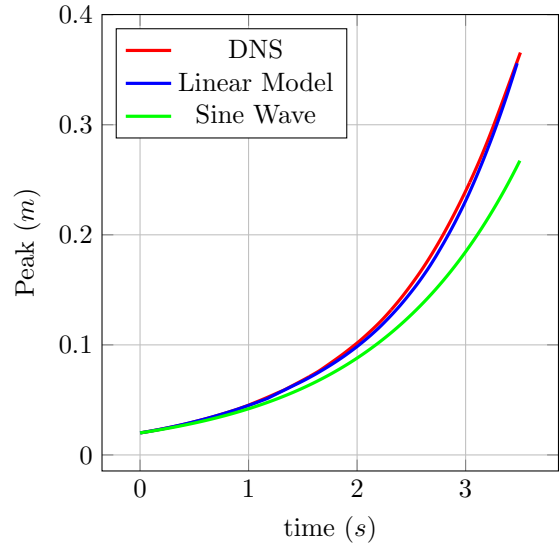


Figure 2. Peak growth comparison

As can be seen in Figure (2), when the amplitude of the perturbation is asymptotically small all three models capture the growth correctly. However, as the disturbance continues to grow into the non-linear regime, the exponentially growing sine wave is unable to capture the growth shown by the DNS and the linear model.

Since the perturbation velocities grow at the same rate as the sine wave, these results are puzzling at first glance. However, the non-linear growth captured by the linear model can be attributed to the use of the projection step. As the interface progresses further into the base flow $U_g(y)$, the projection step corrects for increasingly large base flow velocities.

As a second case, an interface is disturbed with a composition of two wavenumbers. As shown in Figure (3), the interface is perturbed with a disturbance of the form $y = 0.02 \sin(\pi(x - 0.6)) + 0.01 \sin(2\pi x)$.

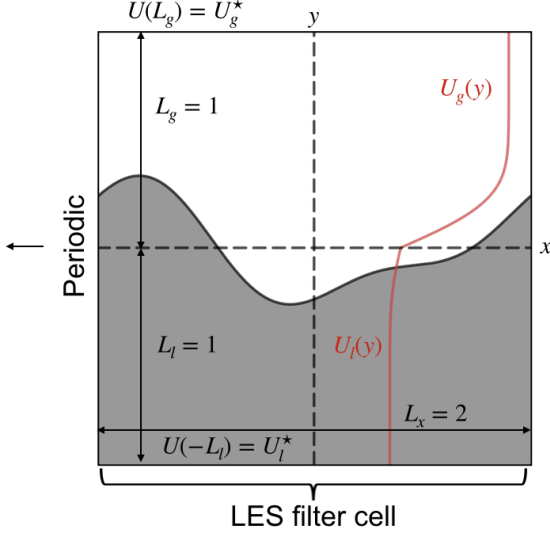


Figure 3. Liquid-gas interface disturbed with a single wavenumber.

Again the simulation is repeated, with the results of the peak growth shown in Figure (4).

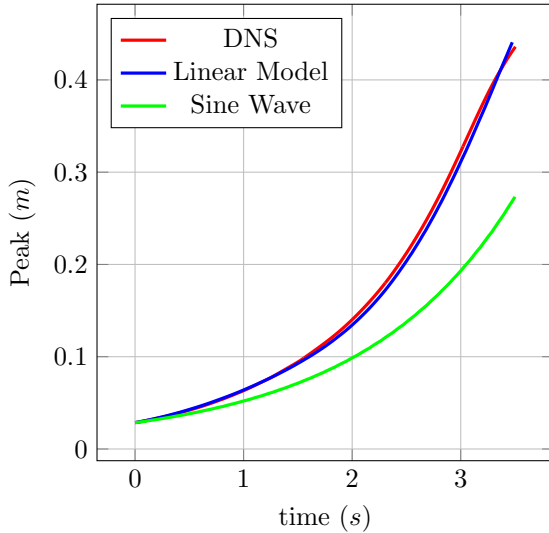


Figure 4. Peak growth comparison

As in the single wave simulation, when the amplitude of disturbance is asymptotically small, all three models are able to capture the growth effectively. However, once the amplitude is sufficiently large and outside the asymptotic regime, the sine wave is unable to capture the growth accurately. The linear model is able to capture some of the effects of non-linear growth observed in the DNS by way of the projection step.

Acknowledgements

We gratefully acknowledge NSF grant 1803657 in support of this work.

References

- [1] M. Gorokhovski and M. Herrmann. *Annual Review of Fluid Mechanics*, 40(1):343–366, 2008.
- [2] E. Labourasse, D. Lacanette, A. Toutant, P. Lubin, S. Vincent, O. Lebaigue, J.-P. Caltagirone, and P. Sagaut. *International Journal of Multiphase Flow*, 33(1):1–39, 2007.
- [3] A. Toutant, E. Labourasse, O. Lebaigue, and O. Simonin. *Computers and Fluids*, 37(7):877–886, 2008.
- [4] M. Herrmann. *Computers and Fluids*, 87:92–101, 2013.
- [5] M. Herrmann. *Journal of Computational Physics*, 227(4):2674 – 2706, 2008.
- [6] T. Boeck and S. Zaleski. *Non-Equilibrium Thermodynamics*, 30(4):215–224, 2005.
- [7] P. Schmid. *Stability and transition in shear flows*. Applied mathematical sciences (Springer-Verlag New York Inc.) ; v. 142. Springer, New York, 2001.
- [8] R. Scardovelli and S. Zaleski. *Annual Review of Fluid Mechanics*, 31(1):567–603, 1999.
- [9] J. Pilliod and E. Puckett. *Journal of Computational Physics*, 199(2):465 – 502, 2004.